UDC 535.317.7:617.7:621.373.826

V.V. Molebny, Dr. Sc.

Principle of local wave front conjugation in ray tracing aberrometry

Проанализированы ошибки измерения, возникающие из-за использования оптической системы глаза как составной части аберрометра, которые в современных скоростных автоматических аберрометрах не учитываются. Статья представляет собой попытку восполнить этот пробел. Выполнено моделирование с помощью программного пакета ZEMAX для метода Хартмана-Шека и метода рейтрейсинга. Показано, что в первом случае ошибки представляют собой простой наклон волнового фронта, который легко исключается при обработке. Во втором случае ошибки имеют более сложные зависимости. Предложен принцип локального сопряжения волнового фронта для рейтрейсинговой аберрометрии, основанный на управлении наклоном входящего в глаз излучения.

Measurement errors, having their origin in using the optical system of an eye as a part of the aberrometer, are analyzed. Today, fast automatic techniques did not care about this kind of errors. The article attempts to fill in the gap. The simulation is made with the ZEMAX software for outgoing (Hartmann-Shack) and ingoing (ray tracing) technologies. It is shown, that in the first case, the errors correspond to simple tilts to be easily excluded at processing. In the second case, the error dependencies are more complicated. The principle of local wave front conjugation for ray tracing aberrometry, based on the control of the tilt of the beam entering the eye, is proposed.

Introduction

Early techniques for measurement of aberrations of the human eye known as a spatially resolved refractometry, used a subjective feedback from the patient [1]. Later, the efforts were undertaken to make the measurements objectively [2]. The tendency to automate the measurements and make them faster resulted in several commercialized technologies. One of them is a Hartmann-Shack wave front sensor [3] whose principle was borrowed from the astronomy and military applications.

In another, ray tracing approach, a point-by-point procedure is applied to probe the eye with a thin laser beam and to get the image of its projection on the retina [4, 5]. The principle of simultaneous projection of regular structure of light on the retina was implemented in the aberrometer [6] based on the principles of Tscherning aberroscope [7]. A skiascopic principle of aberration measurement was implemented in Nidek aberrometer [8, 9].

Physiologically, the most correct is the ray tracing aberrometer since it uses the natural paths of light in the eye projecting the image of outer world on the retina. In the aberrometer using the Hartmann-Shack sensor, the path from the eye is not identical to that along which the optical system of the eye traces the image of the outer world. In Tscherning and skiascopic aberrometers, measuring light is projected on retinal area not corresponding to the area used for vision.

For higher accuracy, several methods and devices were proposed even with the goal to achieve a supernormal vision [10]. Applying this approach to measure the aberrations, the output signal was used to control a wave front conjugation device like a deformable mirror [11] or a phase compensator [12]. The adaptive optic is adjusted in response to a signal generated by the aberration sensor [13] to provide the wave front conjugation.

Some efforts have also been undertaken to design a Hartmann-Shack wave front sensor [14] using low-cost devices such as complementary metal-oxide semiconductor (CMOS) image sensors instead of charge-coupled devices (CCD). Novel architectures known as embedded Hartmann-Shack sensors were recently developed in which the wave front is sensed directly on the image sensor [15]. But the problem of high-cost wave front conjugation with active optics still remains, especially when using photolithographic high spatial density MEMS (Micro-Electro-Mechanical Structure) technologies [16].

Since the coordinates of the elementary mirrors controlling the wave front tilt do not coincide with the coordinates of the eye aperture in which the wave front is measured, the data to control the mirrors should be approximated from the data acquired in the points where the wave front was measured.

1. The eye as a part of the optical system of aberrometer

There are also other sources of error, often thought inevitable, since the optical system of the eye plays a twofold role: as an object of study and

as a part of the aberrometer. This situation creates uncertainty of the results for both ingoing and outgoing techniques. In the ingoing techniques, coordinates of the laser beam on retina are the source of information for subsequent calculations being distorted by the optical system of the eye itself when the coordinates are evaluated through the eye media. In the outgoing techniques, the uncertainty is created due to distortions of the path of the laser beam on its way to retina where it forms a secondary point source of the light. A term "double-pass" was introduced [17] for dealing the situation. It was shown that odd components of the Zernike decomposition compensate themselves on their path back [18]. These considerations are true only if the inward and outward paths are the same.

To resolve the "double-pass" problem, many efforts were made to modify the inward or outward paths in a way to decrease the influence of the pass, which distorts the information [19]. The term was even in use "one and a half pass" [20] to describe the layouts where the influence of the distorting pass was lessened. This term is hardly correct because there is no half passage in either forward or backward direction. As well, the double pass in its strict definition practically never occurs. An interesting approach was tested [21] in which autofluorescence of retinal lipofuscin was used excited by the laser irradiation at shorter wavelength and detection of light signals with the longer wavelengths. This technique causes the same uncertainty of the beam propagation path to the retina with the only exception of different wavelengths in inward and outward directions.

To model the effect of the optical system of the eye as a part of the aberrometer, ZEMAX Optical Design Program (Focus Software, Inc., Tucson, AZ, USA, license EE-13008) was used. The eye was interpreted in paraxial approximation with. aberrations added in the form of Zernike Standard Sag surfaces (*Zernike Std Sag*) with number of terms 37. To simulate the laser beams, circular apertures were placed in the required positions and their *Max Radius* and *Aperture Decenter* were controlled as *Surface Properties*.

1.1. Hartmann-Shack case

The layout of the model of the Hartmann-Shack aberrometer is presented in Fig. 1, where *a* shows the ingoing ray course, and *b* - the outgoing ray course. The radius of the object is set to infinity. The *X*- and *Y-Fields* in the *System* menu are set to zero. Directly after the object, a circular aperture is installed with zero *X*- and *Y-Decenter*. In the results that will be described below, its *Max Radius* was set to 0,02 mm. The retina was simulated with the spherical surface having the radius 12 mm. The coordinates of the spot *R* on the retina, denoted as image height h_{img} , are read off in the *Spot Diagram* window in the *Centroid* mode.

In the outward direction (Fig. 1*b*), the point *R* having the coordinates of the centroid of the retinal spot serves now as a point source of radiation. Image height h_{img} measured when simulating the ingoing ray tracing is set as an object height h_{obj} in the *Fields* group of the *System* menu. At the exit of the eye, in addition to the paraxial and Zernike standard sag surfaces, a circular aperture surface is added. The aperture is denoted as a point *C*. Its position (height) can be varied. Its *Max Radius* is set to 0,02 mm. The rays, leaving the aperture in the point *C*, cross the image (detector) plane in the point *D* having the coordinates (height) h_{det} , which is read off in the *Spot Diagram* window in the *Centroid* mode, in the same manner as in the inward direction.

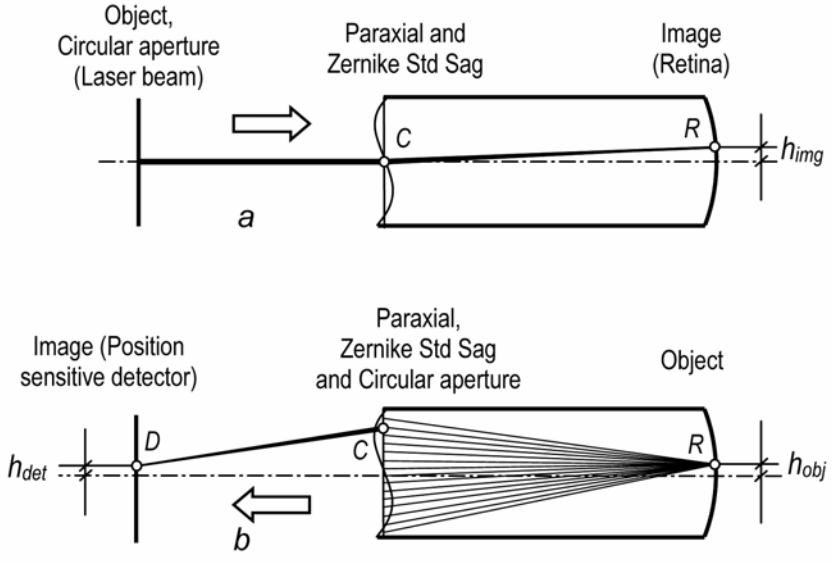

Fig. 1. The layout for modeling the Hartmann-Shack aberrometer

The detector plane is positioned in the back focal plane of the paraxial surface. For the sake of simplification, we excluded the stages of relaying telescope and lenslets, since they do not influence the results except possible linear scaling.

Some examples of the modeling are presented for Z_7, and Z_{17} in Fig. 2. As mentioned above, we used the Zernike standard sags in the form interpreted in the manual [22], which can be easily converted to the form recommended by the ANSI standard [23]. The values for Z_7 and Z_{17} were set to 0,02 mm. The image size was get h_{img} = 0,141 mm for Z_7, and h_{img} = - 0,260 mm for Z_{17}. Then, using these values as h_{obj} = 0,141 mm for Z_7, and h_{obj} = - 0,260 mm for Z_{17}, h_{det} was measured for aperture heights between -4,0 mm and +4 mm. The profiles of h_{det} are shown in Fig. 2*a* and Fig. 2*b* with dotted lines. The solid curves in the same graphs represent the case as if there were no aberration in the inward direction (h_{obj} = 0 mm). Fig. 2*c* and Fig. 2*d* show the difference between the simulated measurements of h_{det} for the cases with and without inward aberrations. This difference corresponds to the error of measurement of each of these Zernike components.

The variations of the error were very small: measured values of h_{det} were $0{,}141^{+0{,}001}_{-0{,}000}$ mm for Z_7 and $-0{,}260^{+0{,}001}_{-0{,}013}$ mm for Z_{17}.

This high constancy of the error means that only the tilt will be induced in the measured data, which is easily excluded at processing. The conclusion for the Hartmann-Shack case is, that there is no problem due to using the eye as a part of the aberrometer.

1.2. Ray tracing case

The layout of the model of the ray tracing aberrometer is presented in Fig. 3, with the ingoing (*a*) outgoing (*b*) ray course. The simulation parameters are set the same as in the Hartmann-Shack case. In the inward direction, the circular aperture can change its position, corresponding to the coordinate of eye probing. In the outward direction, the front focus of the detector lens is set to coincide with the back focus of the paraxial eye. To simplify the simulation, the focal length of the detector lens is set the same as the focal length of the paraxial eye.

The results of modeling of the measurement errors for several Zernike coefficients (Z_7, Z_{17} Z_{19}, Z_{21}, Z_{29}, and Z_{31}) are presented in Fig. 4. Some of error dependencies, like Z_7 and Z_{19}, are smooth, the other ones have higher variability.

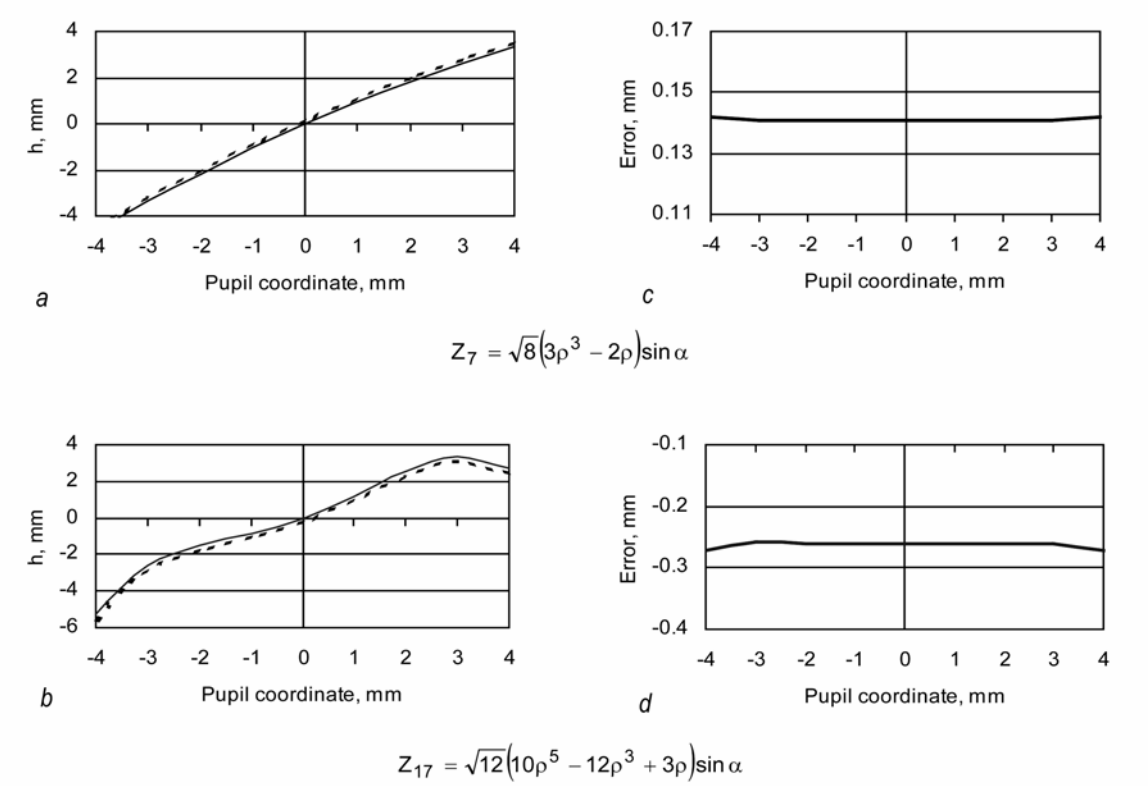

Fig. 2. Height of the object (solid line) and height of the image (dotted line) vs the pupil coordinate in a back projection of the light exiting from the eye with the aberration Z_7 = 0.02 mm (*a*) and Z_{17} = 0.02 mm (*b*). Error of measurement of the aberrations with the Hartmann-Shack aberrometer for Z_7 (*c*) and Z_{17} (*d*)

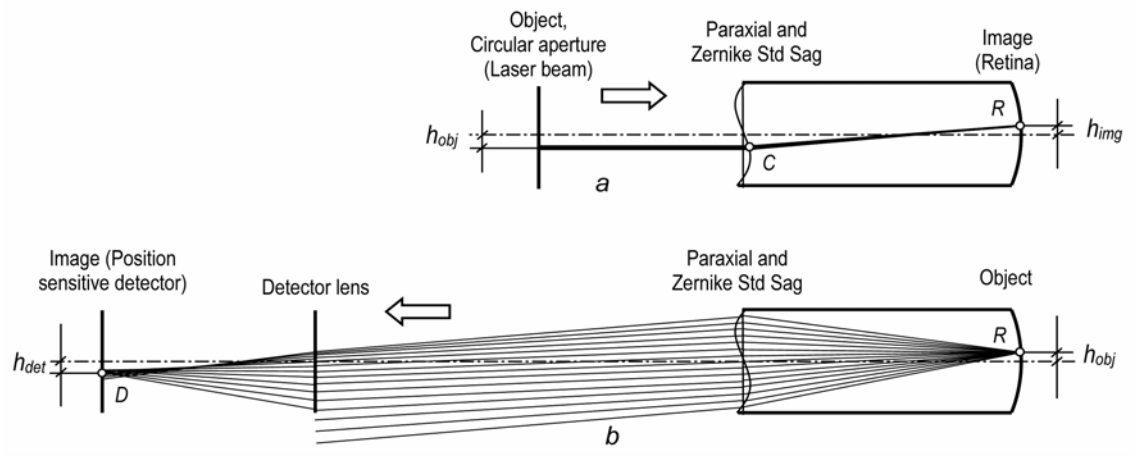

Fig. 3. The layout for modeling the ray tracing aberrometer

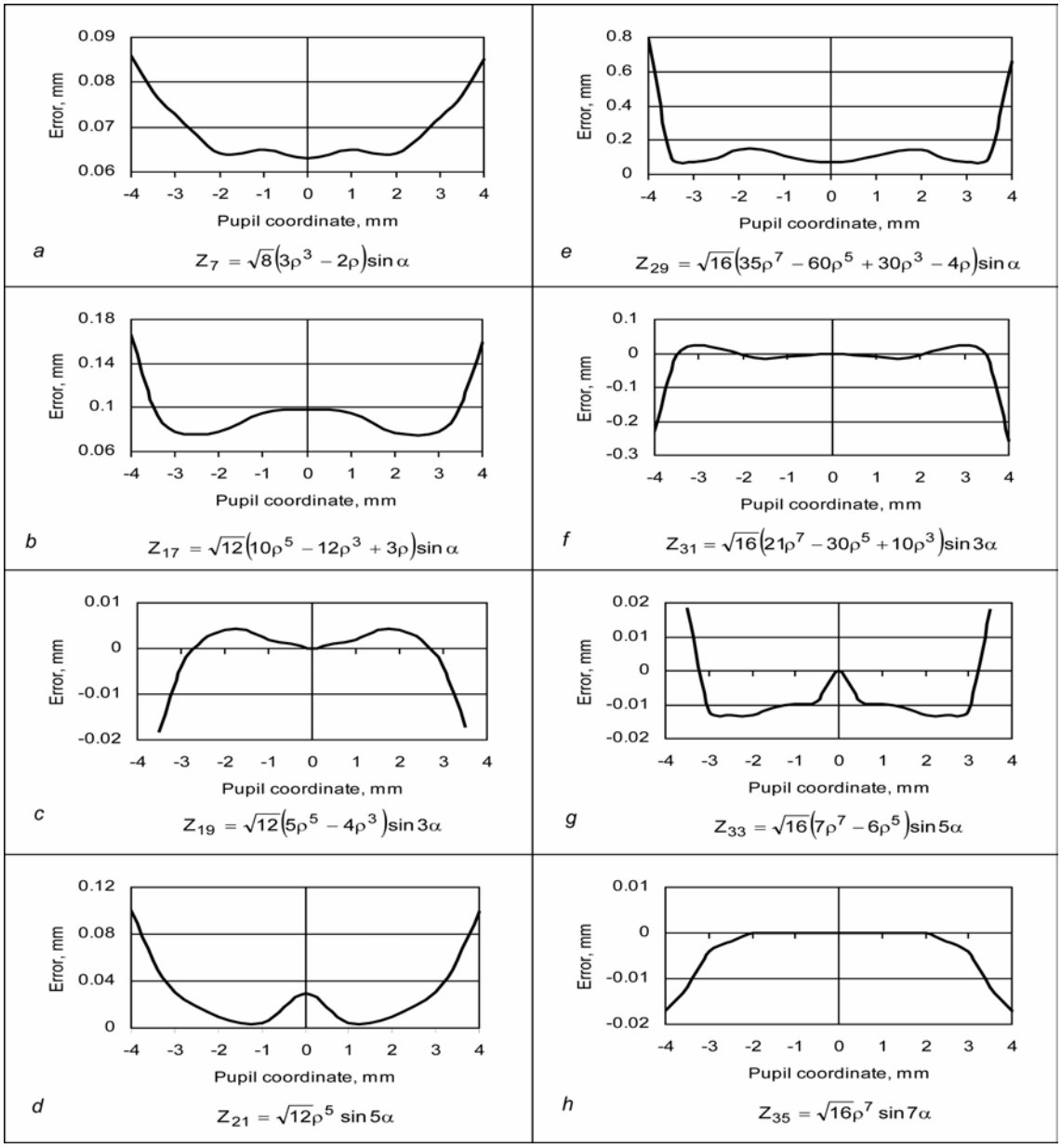

Fig. 4. Error of measurement of the aberrations with the ray tracing aberrometer vs the pupil coordinate in the eye having a single aberration of Zernike standard sag 0,02 mm: *a* - Z_7; *b* - Z_{17}; *c* - Z_{19}; *d* - Z_{21}; *e* - Z_{29}; *f* - Z_{31}; *g* - Z_{33}; *h* - Z_{35}

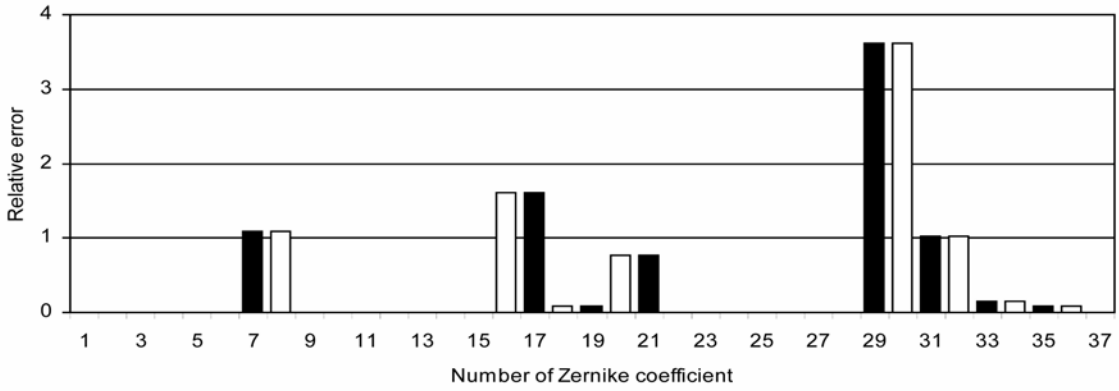

Fig. 5. Relative error of measurement of different Zernike coefficients containing sine multipliers (filled-in columns) and cosine multipliers (empty columns)

The relative root mean square values (RMS values related to the value of the corresponding Zernike coefficient) for some Zernike coefficients containing sine and cosine members are given in Fig. 5.

It is obvious, that the ray tracing technique needs modification to compensate for the measurement errors.

2. The principle of local wave front conjugation

A proposed solution is interpreted by the Fig. 6, where a illustrates a hyperopic type of non-homogeneity, and b - a myopic case. In the standard ray tracing mode [4], the beam exits the deflector center of deflection in the point O1 and enters the eye in parallel to the optical axis of the instrument at the height h_1 crossing the anterior surface of the cornea in point C. The beam hits the retina in point R_h at the height d_h from the central point R for the hyperopic type of non-homogeneity. For the myopic type, the retina is hit in the point R_m at the height d_m.

To solve the problem of wave front conjugation in the point C of the entrance into the eye, the tilt of the beam inside the eye is to be changed from φ_1 to φ_2. This can be done by changing the height of the beam at the deflector center of deflection from h_1 to h_2 and inclining the beam by the angle β_h for the case of hyperopia or by β_m for myopia. It means that the height of the beam in the center of deflection must be shifted from point O_1 to point O_2.

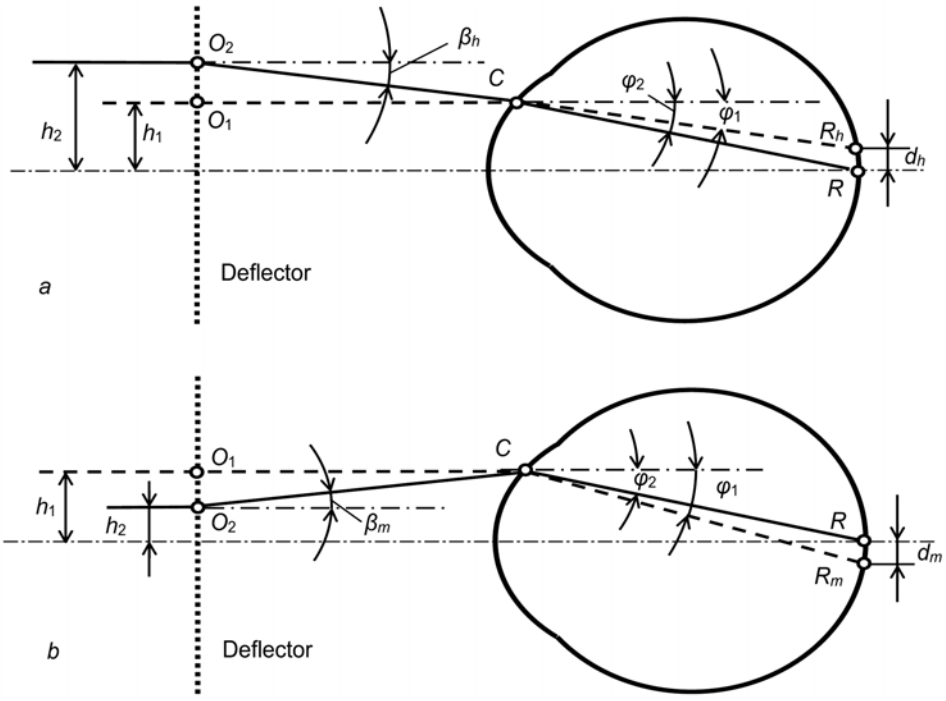

Fig. 6. Principle of the local wave front conjugation for the errors of the hyperopic type (*a*) and of the myopic type (*b*)

It can be done with an additional deflector and a collimating lens. Since the information on tilts β_h or β_m is got with errors, the correction of the position of R_h or R_m will not result in achieving zero values of d_h or d_m, in the very first correction, and another iteration may be necessary, similarly to the systems with the simultaneous total wave front conjugation. Fig. 7 illustrates the results of the consecutive wave front conjugation procedures showing the retinal spot diagrams after the initial probing (*a*), the first (*b*) and the second (*c*) iterations.

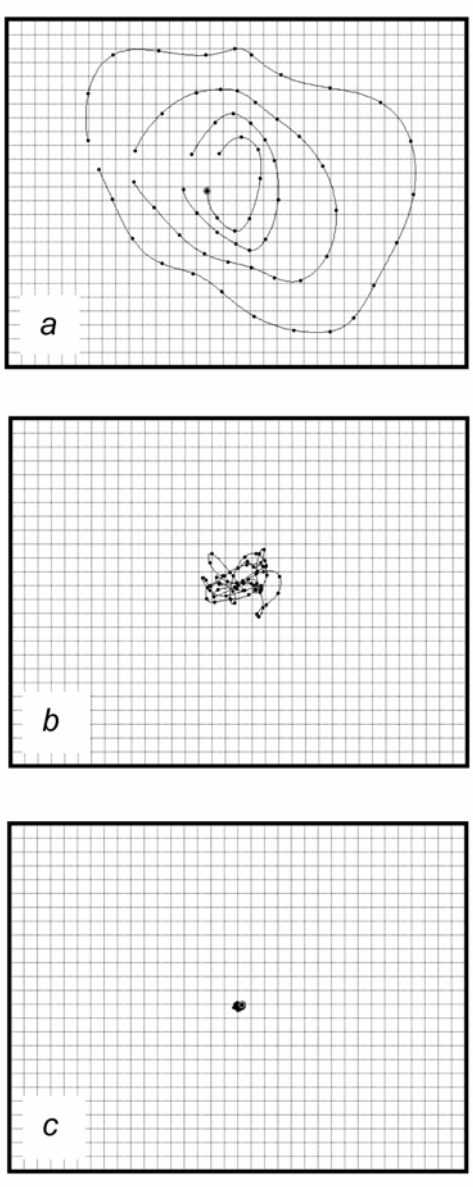

Fig. 7. Retinal spot diagrams:
***a* - without local wave front conjugation;**
***b* - with the local wave front conjugation, first iteration;**
***c* - with the local wave front conjugation, second iteration**

Conclusion

The proposed principle of local wave front conjugation allows decreasing of the measurement error by an order per iteration. Depending on the type of aberration, it means that the error from 20% will be reduced to 2% after the first iteration, and to 0,2% after the second iteration. In most cases, a single iteration can be enough. When the level of measurement noise is low and the uncertainties following from the extrapolation procedures are lessened due to a high number of probing points, the second iteration may solve the problem with even higher accuracy.

References

1. *С. М. Смирнов* Измерение волновой аберрации глаза. Биофизика. 1961, № 6, с. 776-794.
2. *R. H. Webb*, C. M. Penney, K. P. Thompson. Measurement of ocular local wavefront distortion with a spatially resolved refractometer. Applied Optics. 1992, Vol. 31, No. 19, pp. 3678-3686.
3. *J. Liang*, B. Grimm, S. Goelz, J. F. Bille. Objective measurement of wave aberrations of the human eye with the use of a Hartmann-Shack wave-front sensor. Journal of the Optical Society of America: A. 1994, Vol. 11, No. 7, pp. 1949-1957.
4. *V. V. Molebny*, I. G. Pallikaris, L. P. Naoumidis, I. H. Chyzh, S. V. Molebny, V. M. Sokurenko. Retina ray-tracing technique for eye-refraction mapping. Proceedings of the SPIE, 1997, Vol. 2971, pp. 175-183.
5. *R. Navarro*, E. Moreno-Barriuso. Laser ray-tracing method for optical testing. Optics Letters. 1999, Vol. 24, No. 14, pp. 951-953.
6. *P. Mierdel* et al. Ocular optical aberrometer for clinical use. Journal of Biomedical Optics. 2001, Vol. 6, No. 2, pp. 200-204.
7. *M. Tscherning*. Die monochromatischen Aberrationen des menschlichen Auges. Zeitschrift für Psychologie und Physiologie der Sinnesorgane. 1894, Bd. 6, S. 456-471.
8. *M. Fujieda*. Ophthalmic measurement apparatus having plural pairs of photoreceiving elements. U.S. Patent 5,907,388. 25.05.1999.
9. *S. MacRae*, M. Fujieda. Slit skiascopic-guided ablation using the Nidek laser. Journal of Refractive Surgery, 2000, Vol. 16, No. 5, pp. S576- S580.
10. *J. Liang*, D. R. Williams, D. T. Miller. Supernormal vision and high-resolution retinal imaging through adaptive optics. Journal of the Optical Society of America: A. 1997, Vol. 14, No. 11, pp. 2884-2892.

11. *D. R. Williams*, J. Liang. Method and apparatus for improving vision and the resolution of retinal images. U.S. Patent 5,777,719. 07.07.1997.
12. *B. M. Levine*, A. Wirth, C. H. Knowles. Ophthalmic instrument with adaptive optic subsystem that measures aberrations (including higher order aberrations) of a human eye and that provides a view of compensation of such aberrations to the human eye. U.S. Patent 6,709,108. 23.03.2004.
13. *C. E. Campbell*. Eye refractor with active mirror wavefront sensor. U.S. Patent 7,128,416. 31.10.2006.
14. *T. Nirmaier*, G. Pudasaini, J. Bille. Very fast wave-front measurements at the human eye with a custom CMOS-based Hartmann–Shack sensor. Optics Express. 2003, Vol. 11, No. 21, pp. 2704-2716.
15. *J. Vaillant*. Wavefront sensor architectures fully embedded in an image sensor. Applied Optics. 2007, Vol. 46, No. 29, pp. 7110-7116.
16. *F.-Y. Chen*, W.-Y. Wang, Y.-H. Chang, T.-Y. Wu. Surface MEMS mirrors with oxide spacers. U.S. Patent 7,205,176. 17.04.2007.
17. *D. R. Williams*, D. H. Brainard, M. J. McMahon, R. Navarro. Double-pass and interferometric measures of the optical quality of the eye. Journal of the Optical Society of America: A. 1994, Vol. 11, No. 12, pp. 3123-3135.
18. *P. Artal*, S. Marcos, R. Navarro, D. R. Williams. Odd aberrations and double-pass measurements of retinal image quality. Journal of the Optical Society of America: A. 1995, Vol. 12, No. 2, pp. 195-201.
19. *V. N. Kurashov*, V. V. Molebny, A. V. Kovalenko, I. G. Pallikaris, L. P. Naoumidis. Double-pass wave model in eye aberrations study. Proceedings of the SPIE, 1997, Vol. 3192, pp. 243-248
20. *R. Navarro*. Private communication. 2nd Aegian Summer School in Visual Optics, Santorini, Greece, July 2003.
21. *L. Diaz* Santana and J. C. Dainty. Single-pass measurements of the wave-front aberrations of the human eye by use of retinal lipofuscin autofluorescence. Optics Letters. 1999, Vol. 24, No. 1, pp. 61-63.
22. *ZEMAX*. Optical Design Program. User's Guide. Version 10.0. Focus Software, Inc., Tucson, AZ. 2001, 472 pp.
23. *Methods* for reporting optical aberrations of eyes. American National Standard for Ophthalmics: ANSI Z80.28-2004. American National Standards Institute, Inc. 14.05.2004, 36 pp.